

IMPROVEMENT THE CELL VIABILITY OF METALLIC IMPLANTS BY ALOE VERA ADDITIONS WITH NATURAL HYDROXYAPATITE

Noor Mohammed^{*1}, Fatimah J. Al-Hasani², Aseel B.AL-Zubaidi³

¹College of Engenering , Uruk University, Baghdad, Iraq.

^{2&3} Materials Engineering Department, University of Technology, Baghdad, Iraq.

mae.19.16@grad.uotechnology.edu.iq

Abstract A bio-organic coating was created familiar the biological system by extracting hydroxyapatite from the original natural sources, including eggshells, fish bones, and cockle shells. Natural polymer extract from Aloe Vera, it was used as the basic material for the coating and natural hydroxyapatite was added. In order to reduce the impact of metallic within the biological system and improvement the cell viability of metallic implants.

 Crossref  10.36371/port.2022.3.7

Keywords: biomaterials, natural hydroxyapatite, eggshell, fish bone, cockle shell, natural polymer, aloe Vera, MTT assay, the cell viability.

1. INTRODUCTION

A new In recent years, the interaction between biomaterials and renewable resources has offered a window of opportunity for the creation of fresh, sustainable emerging techniques. In the distant past, people used biomaterials without being aware of it. Their production from sustainable resources has received a lot of attention recently, motivated by the desire to create increasingly more sustainable alternatives to traditional materials. Because they represent the path to a more sustainable future, biocompatible materials with attributes similar to existing materials are becoming more and more important for the pressing need for sustainable energy development.[1]

In the not too distant future, bioprocesses with innovative environmentally friendly methods and viewpoints that support a switch from traditional production routes to sustainable alternatives, as envisioned in the UN 2030 Agenda for Sustainable Development, will play a significant role. The transition to sustainable processes is concentrated on the creation of biorefineries, which produce valuable compounds from biomass, as well as on the application of new technologies based on renewable resources (from both marine and particular terrestrial ecosystems), agricultural wastes, and industrial byproducts. With the sustainable bioconversion of such feedstocks or raw materials into a

variety of high-value products, sub-products will be valued, which will benefit the economy and the environment.[2]

After blood, bone is the second most often implanted tissue in the human body. Numerous bone graft scaffolds that are currently accessible have established the use of bone replacement material to treat, repair, or supplement skeletal injuries. The scaffold materials' capacity to combine mechanical stability, biological activity, and affordability for these applications is still being researched. The high cost of biological materials is caused by their costly chemical precursors or synthetic processes. Due to rejections in the human system, the bioactivity of replacement material is also a major concern.[3]

Chemically speaking, hydroxyapatite, or $\text{Ca}_{10}(\text{PO}_4)_6(\text{OH})_2$, is identical to the mineral that makes up bones and teeth and is one of the few bioactive substances, hence it will In orthopaedic, dental, and maxillofacial applications, materials that assist bone ingrowth and osseointegration are employed.

To enhance the surface qualities of metallic implants, particularly those made of titanium alloys and stainless steels, hydroxyapatite coatings are frequently used. When substantial parts of bone have to be removed or when bone augmentations are necessary, it can be used as powders, porous blocks, and hybrid composites to cover bone flaws or cavities (e.g. dental applications).[4]



This paper examines the improvement of the performance of biomaterials used in bone implants and their manufacture from environmentally friendly materials that support the concepts of sustainability.

In order to reduce the effect of the metallic within the biological system and improve the viability of the cultured mineralized cells, an organic bio-coating of aloe Vera and natural hydroxyapatite was used, as they are familiar materials for the biological system and thus work to reduce the effect of the metallic on it.

2. EXPERIMENTAL WORK

2.1 Natural Hydroxyapatite Powder Extraction

A After drying for an hour at 100 °C and calcining for two hours at 250 °C, hydroxyapatite was isolated from eggshells. After that, the material was ground and smoothed until it was a fine powder. Fish bones were dried for one hour at 100 °C before being calcined at 250 °C for two hours to extract the hydroxyapatite. Then comes the grinding step to produce a fine powder. Cockle shells were dried for two hours at 100°C, then ground to extract the hydroxyapatite.

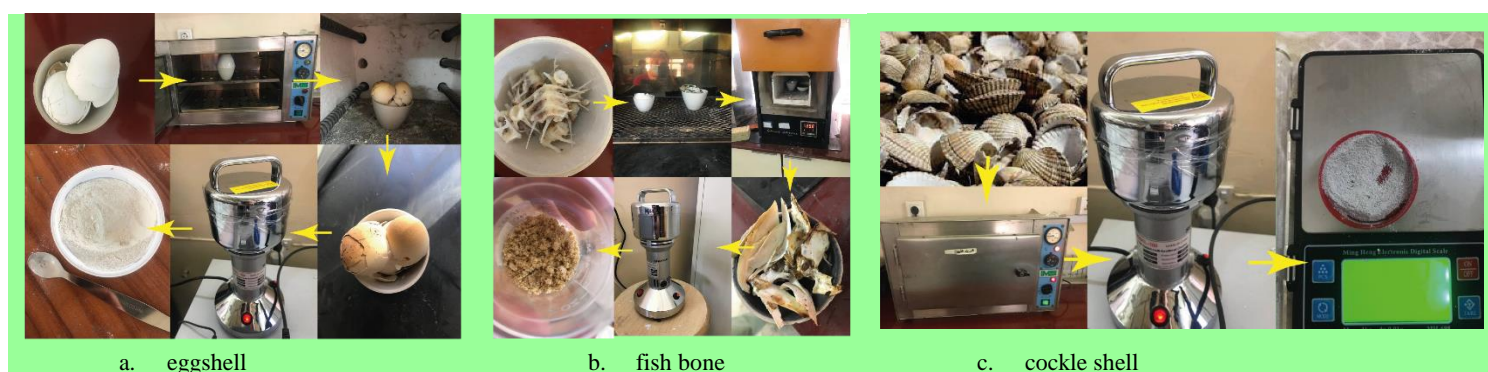


Figure 1 extraction natural hydroxyapatite

2.2. Preparation Of Natural Polymer

Aloe Vera gel and sodium alginate are combined to create a natural hybrid polymer. To manually extract the aloe Vera, a clean, sharp knife was used. It was then disinfected with 99 percent pure ethanol after being rinsed with DI water and left to air dry.

To further homogenize and overlap the leaf gel, it was first agitated for ten minutes using a mechanical mixer. In order to achieve even higher homogeneity, it was slowly stirred for a half-hour using a magnetic stirrer. After that, it was thoroughly mixed for a half-hour using an ultrasonic

machine. Finally, it was left for ten minutes to allow air bubbles to rise to the top. Sodium alginate polymer was added to aloe vera gel to increase its mechanical strength and adhesive surface because aloe vera gel's mechanical weakness makes it difficult for it to adhere to the surface of an implant. Water was added to the compound after it had been diluted to 5% weight in order to make polymer alginate. The aloe Vera polymer was then added to the magnetic stirrer and swirled for 30 minutes at a 2: 8 ratio utilizing volume ratio calculations. There was a 10-minute break after another 30 minutes of ultrasonic mixing.



Figure 2 preparation natural polymer .

2.3 Preparation Of The Whole Composites Coating Materials

preparation of two different composite coating material groups A and B. To form the polymeric matrix, the composite solution in Preparation group A was first blended with 5% weight of HA particle. The composite coating solution was first stirred with a magnetic stirrer for 30 minutes, and then stirred again with ultrasonic for another 30 minutes. Then, in preparation group B, the composites solution was made by adding 5%wt HA (extract from various natural sources) and 5%wt mastic, which was made by crashing mastic for 15 minutes. The coating solution was stirred for 30 minutes with a magnetic stirrer, then again for 30 minutes with ultrasound. Finally, both groups of composite coating materials are ready for the dip-coating process.

2.4 Surface Preparation By Chemical Treatment

The substrate is 5 cm by 3 mm in size and is composed of 316L stainless steel. It is possible to increase surface roughness and make sure that the implant surface and polymeric covering layer adhere to one another effectively by eliminating scales and oxide from the substrate. Hydrofluoric acid is employed in an acidic treatment. Hydrofluoric acid is used in an acidic procedure. First, a hydrofluoric solution was created by dissolving five 0.1 g solid acid particles in 40 mm of water. The samples were then thoroughly cleaned, submerged for five minutes, and given thirty minutes to dry naturally. Then, it was subjected to hydraulic acid at a concentration of 0.5 ml molar for four hours at 40 C. To increase biological activity, the samples underwent an alkaline treatment using sodium hydroxide solution at a concentration of 10 mM for 24 hours at 60 C. After that, the samples were dried and rinsed with distilled water. The proper temperature was also maintained while the samples were being handled. Using a water bath, the temperature of the samples was kept at the appropriate level.



Figure 3 proration surface by chemical treatment

5-2 Samples Coating

The implant sample was coated using the dip coating technique. A natural hybrid polymer and hydroxyapatite, which can be found in a variety of natural sources, were used to create the dipping solution (eggshell, fish bone, and cockle shell). The procedure involves immersing a stainless steel sample in the solution for one minute, taking it out, holding it for ten minutes, and repeating the procedure ten times. Each sample was submerged for a total of two hours and fifty minutes.

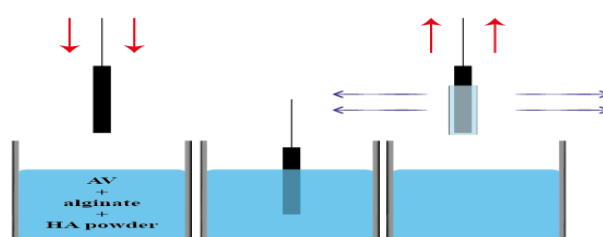


Figure 4 coating samples by whole composition materials

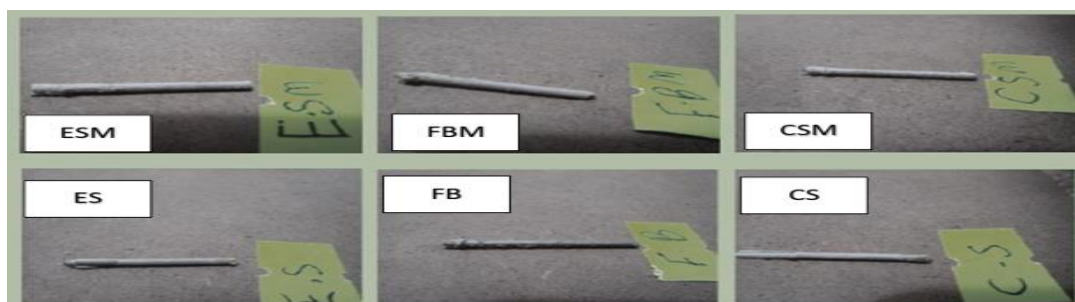


Figure 5 samples after coating

Table 3.1 Sample code names

SAMPLE	Name
SS	Stainless steel sample without any treatment or coating
ES	Stainless steel sample after treatment and coating with natural polymer and hydroxyapatite from eggshell
FB	Stainless steel sample after treatment and coating with natural polymer and hydroxyapatite from fishbone
CS	Stainless steel sample after treatment and coating with natural polymer and hydroxyapatite from cockleshell
ESM	Stainless steel sample after treatment and coating with natural polymer and hydroxyapatite from eggshell with mastic
FBM	Stainless steel sample after treatment and coating with natural polymer and hydroxyapatite from fishbone with mastic
CSM	Stainless steel sample after treatment and coating with natural polymer and hydroxyapatite from cockleshell

3. RESULTS AND DISCUSSIONS

3.1 Field emission scanning electron microscopy (FESEM)

Figure (6) shows a FE-SEM image for sample SS to compare surface changes with other samples after treatment and coating. The surface is uneven because it has peaks and grooves. Few, irregularly spaced peaks and grooves with sizes between 1.4 and 467 nm are present on the surface.

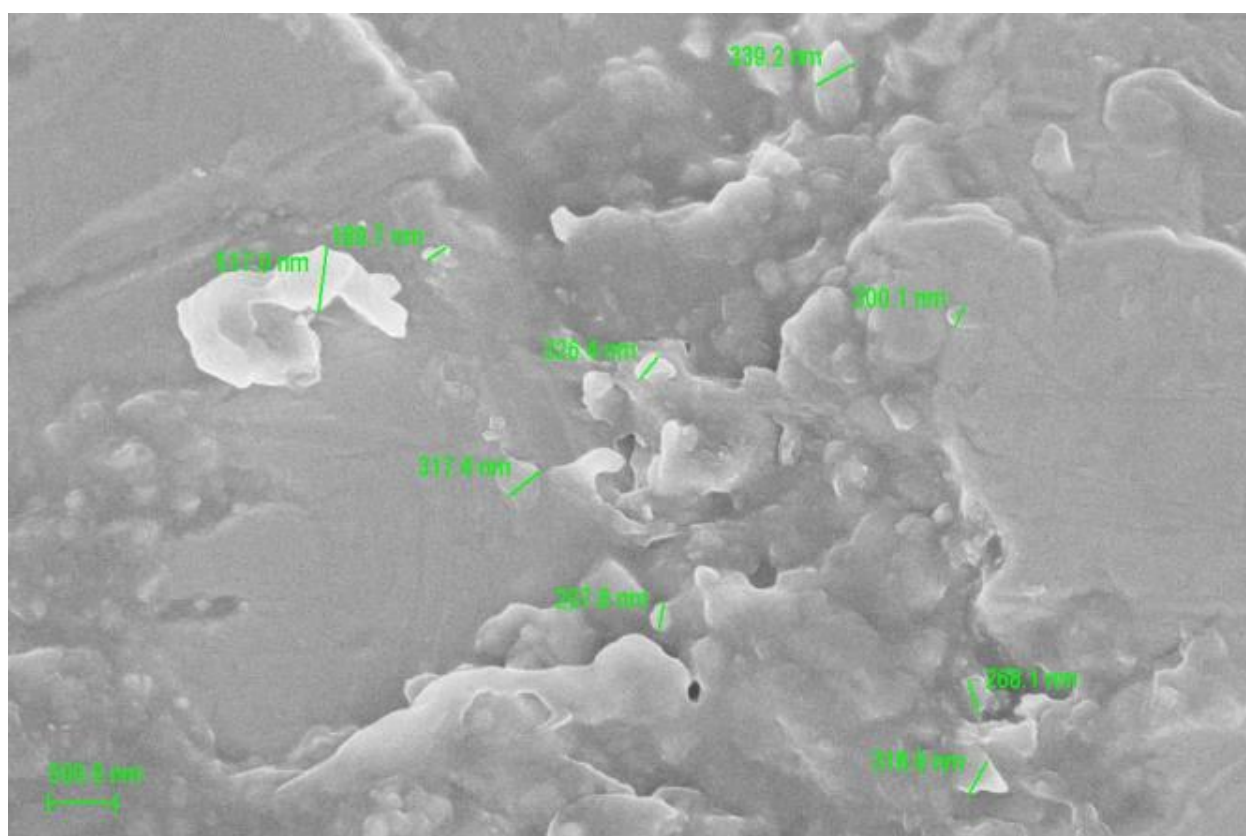


Figure 6 Field emission scanning electron microscopy (FESEM) for sample (SS)

The FE-SEM picture for sample ES is shown in Figure (7). (stainless steel after coating with natural polymer and hydroxyapatite extract from eggshell). The coating's uneven and accumulative dispersion across the surface is what gives

it its appearance. The coating substance also fills in the grooves that already exist on the stainless steel surface. As a result, new grooves and peaks are produced as the diameters increase from 1 nm to 35 nm, increasing in number but

Figure shows the FE-SEM picture for sample CS (9). (stainless steel after being coated with a natural polymer and cockleshell hydroxyapatite extract). Due to the materials' different granular sizes, which range from 3 μm to 48 nm, there are many grooves and peaks of different sizes, which results in the production of highly visible grooves and peaks and, as a result, a high concentration of sites for cell growth and

adhesion. The surface's shape exposes a thick layer of coating material that is dispersed unevenly and in accumulations and agglomerations of various sizes. It is also noted that the grain concentration and distribution generated the shape of very big grooves, resulting in a bigger surface area, in addition to the size diversity, which created a wide range of different surface areas inside the crests and grooves.

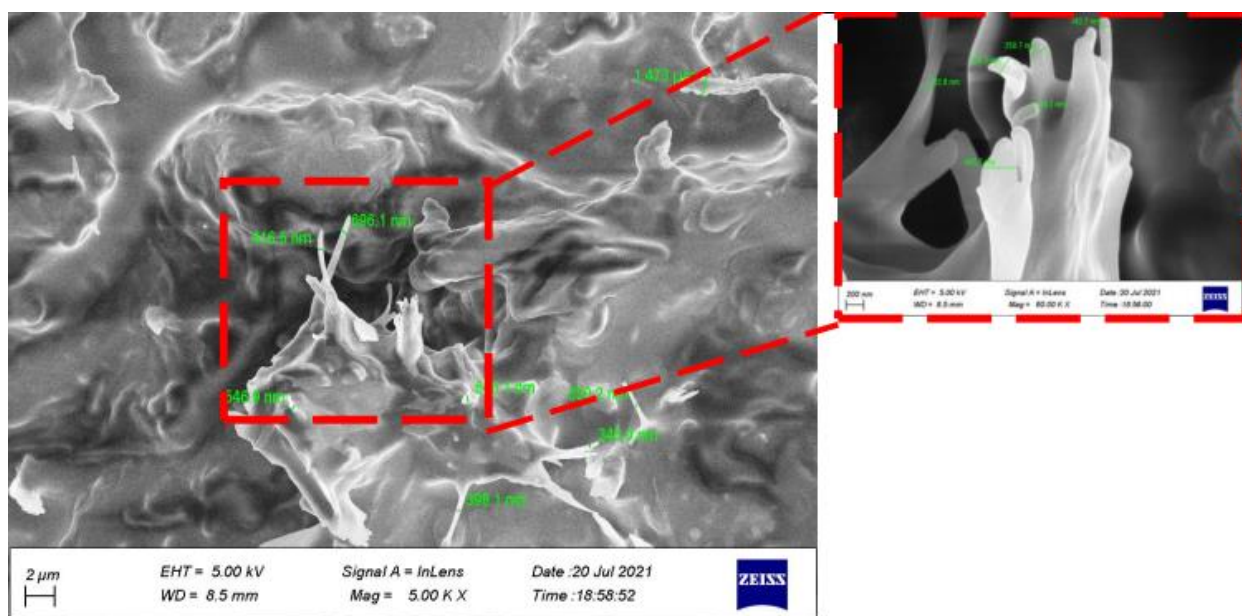


Figure 8 Field emission scanning electron microscopy (FESEM) for sample (CS)

Figure shows the FE-SEM image for the sample ESM (10). (Stainless steel with mastic after coating with natural polymer and eggshell extract hydroxyapatite). The smaller mastic granules spread over and between the grooves and peaks formed by the hydroxyapatite granules, creating new peaks

and grooves of smaller sizes. The sizes range from 3 μm to 51 μm . High contrast is produced as a result, and a better surface structure is provided for cell spread and adhesion to the implant.

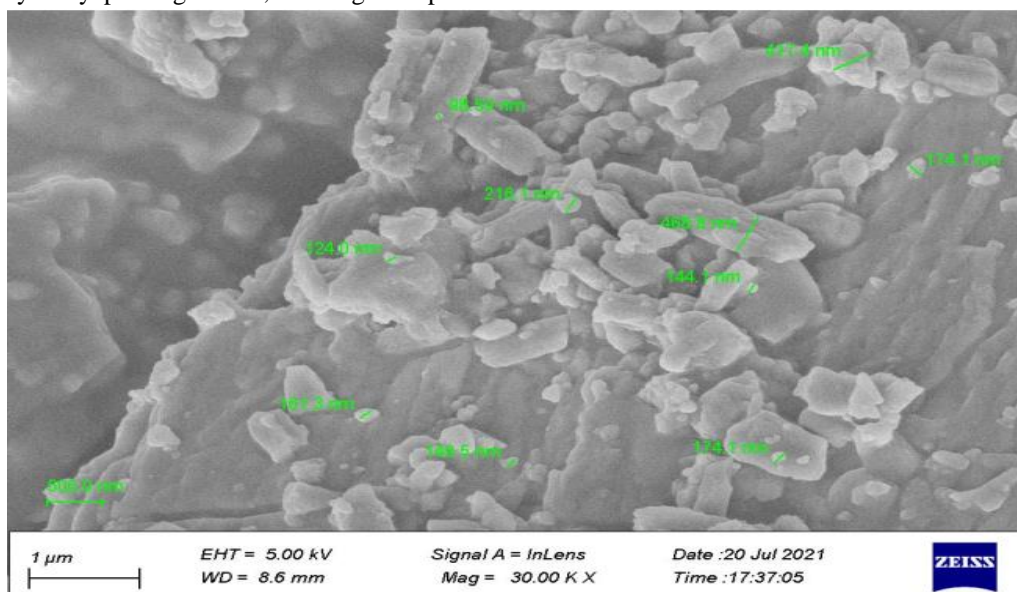


Figure 9 Field emission scanning electron microscopy (FESEM) for sample (ESM)

The hydroxyapatite grains were evenly distributed throughout the natural polymer, proving that the mixing and coating procedure was a great success.

Mastic was able to improve the morphology of the surface since it is one of the few materials that, when combined with other materials, maintains its original qualities and does not acquire those of the other material.

The morphology of the surface has also been improved by the addition of mastic.

This demonstrates how the surface shapes produced by the different hydroxyapatite forms are perfect for cell growth and adhesion to their surface.

Table (2) shows the average particle size of the materials based on the FE-SEM findings.

Table (2) shows the Average particle size of each material

Material	Average of particle size
SS	1.4 μ m to 467 nm
ES	1 μ m to 35 nm,
FB	1 μ m to 261 nm.
CS	3 μ m to 48 nm,
ESM	3 μ m to 51 nm,
FBM	2 μ m to 51 nm,
CSM	2 μ m to 48 nm

3.2 Fourier Transform Infrared (FTIR)

The results FTIR of the samples show the peaks that represent the effective aggregates as a result of mixing natural hydroxyapatite shown in the table below. Table 3. Display the FTIR main peaks for various coating materials and chemical groups.

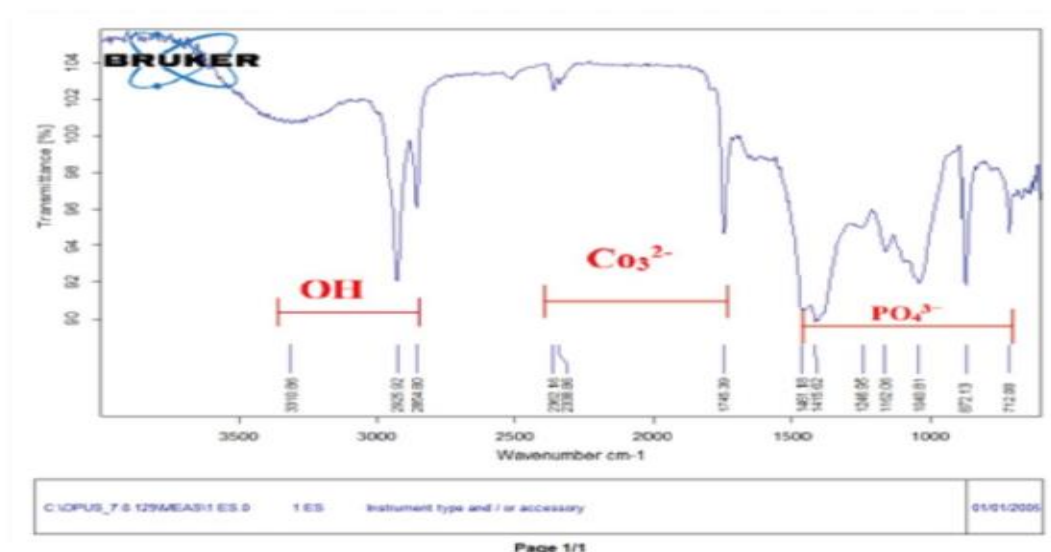
Table 3 Show main peaks for FTIR for a different type of coating material

Chemical group		Wave number cm-1				
ES			CS	ESM	FBM	CSM
PO43-					1241.48	
					1179.12	
					1151.5	1379.11
					1129	1243.95
	1246.95	1378.07	1377.81		1104.76	1162.76
	1102.06	1239.76	1245.9	1263.62	1029.95	1115.66
	1040.81	1159.09	1164.18	1024.76	960.37	1093.88
	872.13	1092.96	1094.78	873.63	906.95	1040.76
	712.08	1029.78	1043.15	711.88	881.14	875.7
		877.6	854.49	649.9	824	721.58
CO32-		722.82	721.87		741	
					650.73	
		1743.91				
		1633.52	2361.75			1745.88
	1745.39		2341.04	1796	1692.7	1673.8
	1461.18	1567.49	1745.71	1730.34	1458	1637.4
	1415.95	1501.77	1462.28	1587.67	1409.7	1463.6
OH		1460.73	1417.3	1405.08		
		1416.88				
	3310	3323.78				3350.49
	2925.92	2924.24	3380.99		2927.5	2926.14
	2854.8	2854.1	2926.46	3323.85	2868.17	2855.04
	2362.16	2349	2854.95	2929.73	2360.7	2361.8
	2333.86					2338.4

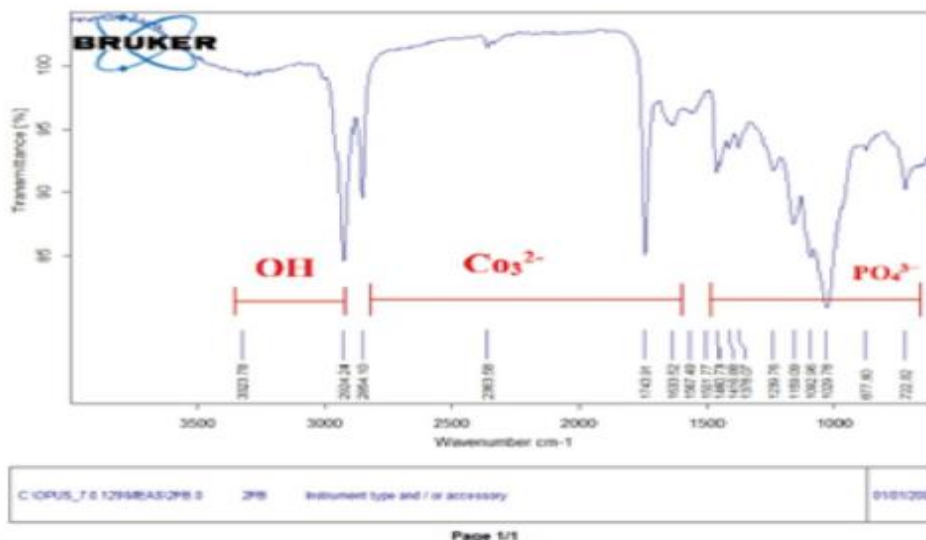
chemical group when comparing the results of the samples obtained from the results of FTIR for samples of natural crushed hydroxyapatite as in FTIR result, with the natural hybrid compound resulting from mixing natural hydroxyapatite with the natural polymer formed with alginate and aloe Vera. The peaks show the effective aggregates of hydroxyapatite and notice a deviation in some peaks with the emergence of other strong peaks indicating the emergence of hydroxyl and carboxylate, which indicates the presence of aloe Vera and alginate. indicate the emergence of the active

group(OH) hydroxyl, which is the result of the presence of the natural polymer (aloe Vera + alginate) with the expected peaks depending on the source[5], which shows that mixing aloe Vera with alginate There is no effect on the amount of infrared absorption, as the appearance of the hydroxyl group and the carboxyl group are in the form of sharp peaks, and the samples that were examined showed the appearance of these peaks in the expected places and the values are very close, and this indicates the interaction of aloe Vera and alginate and the emergence of their effective groups.

ES FILM



FB FILM



CS FILM

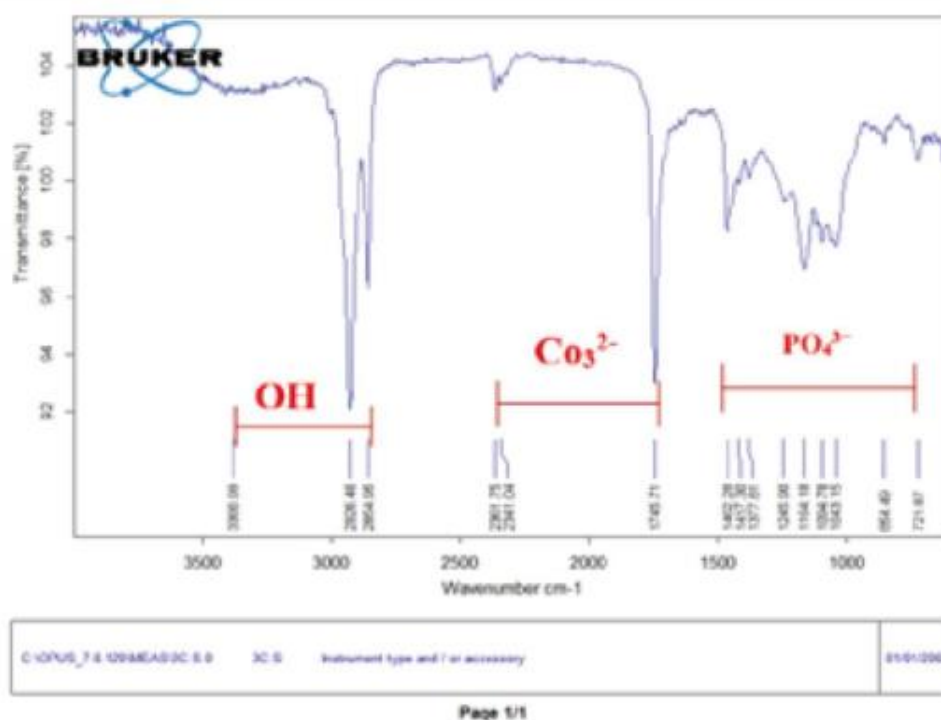


Figure 11 show the FTIR test for ES FILM, FB FILM, and CS FILM

The figure 14 shows the image of the results of FTIR for the natural hybrid compound consisting of natural hydroxyapatite extracted from eggshells, fish bones and cockle shells and mastic. Where the main peaks appear showing the main active groups of hydroxyapatite and the natural polymer, in addition to the appearance of the

carboxylate group in the form of a strong peak indicating the presence of the mastic substance, which contains antibacterial properties, and is a natural resin, it can be identified by the appearance of the active carboxyl group at the peaks of 1700, as shown by the examination below of the mastic substance figure (mastic), this is agree with the source[6].

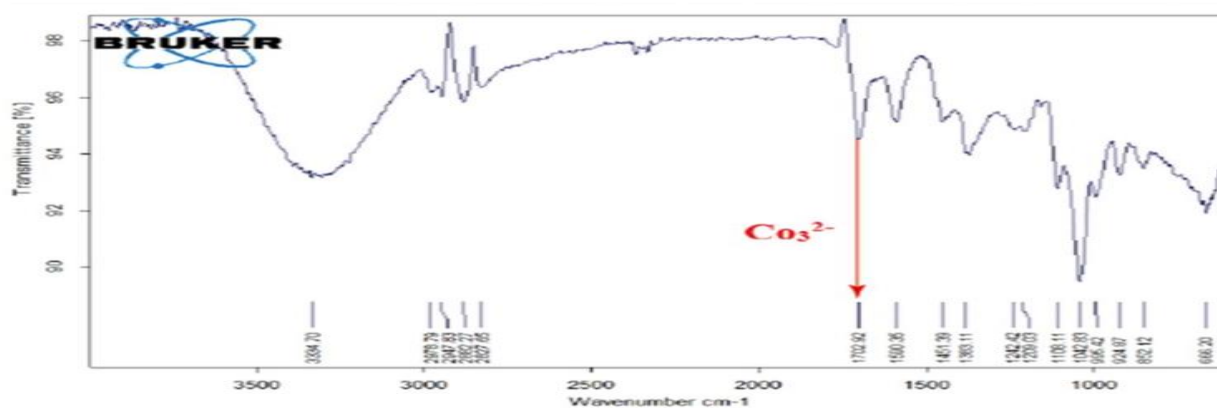
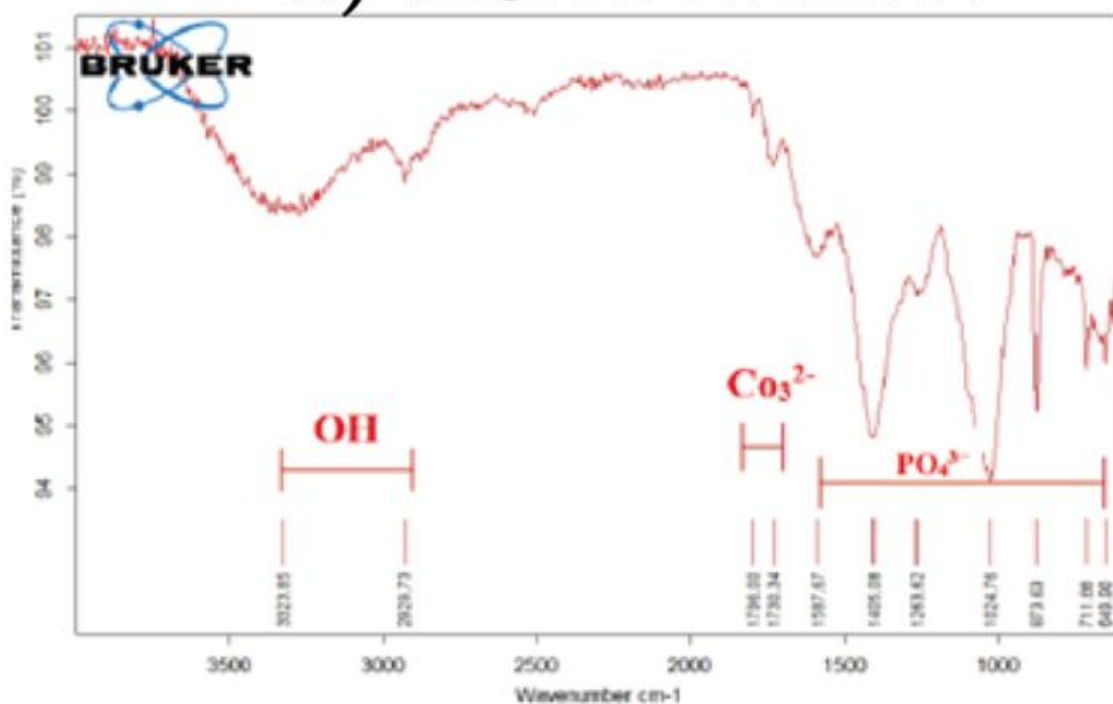
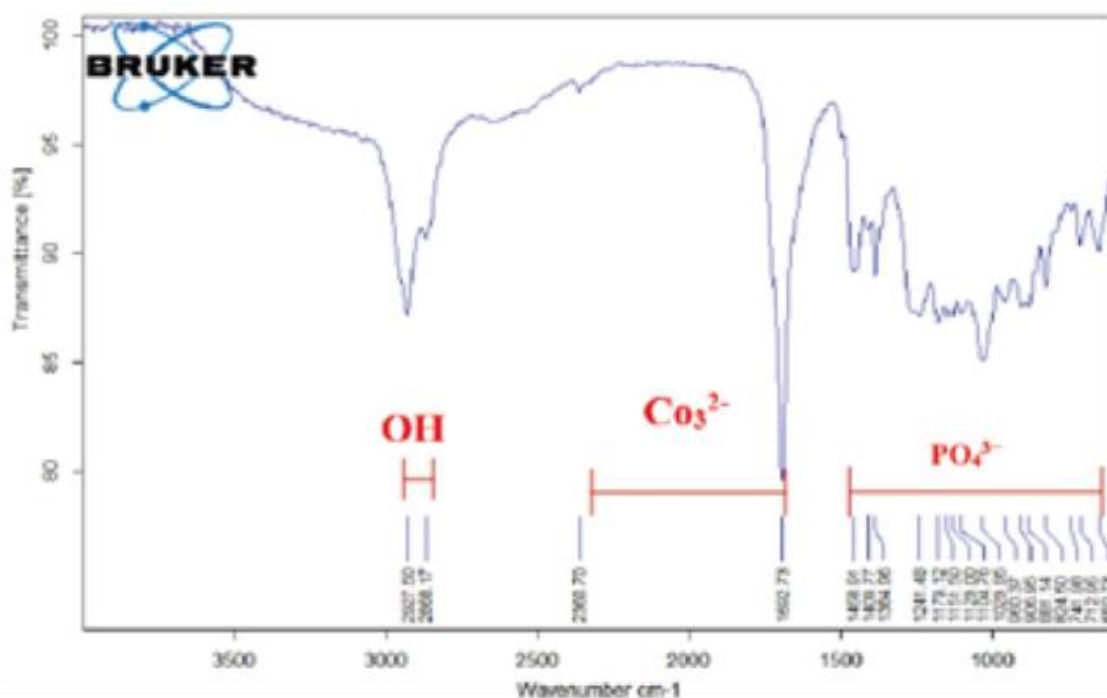


Figure 12 show the FTIR test for mastic

a) ESM FILM



a) FBM FILM



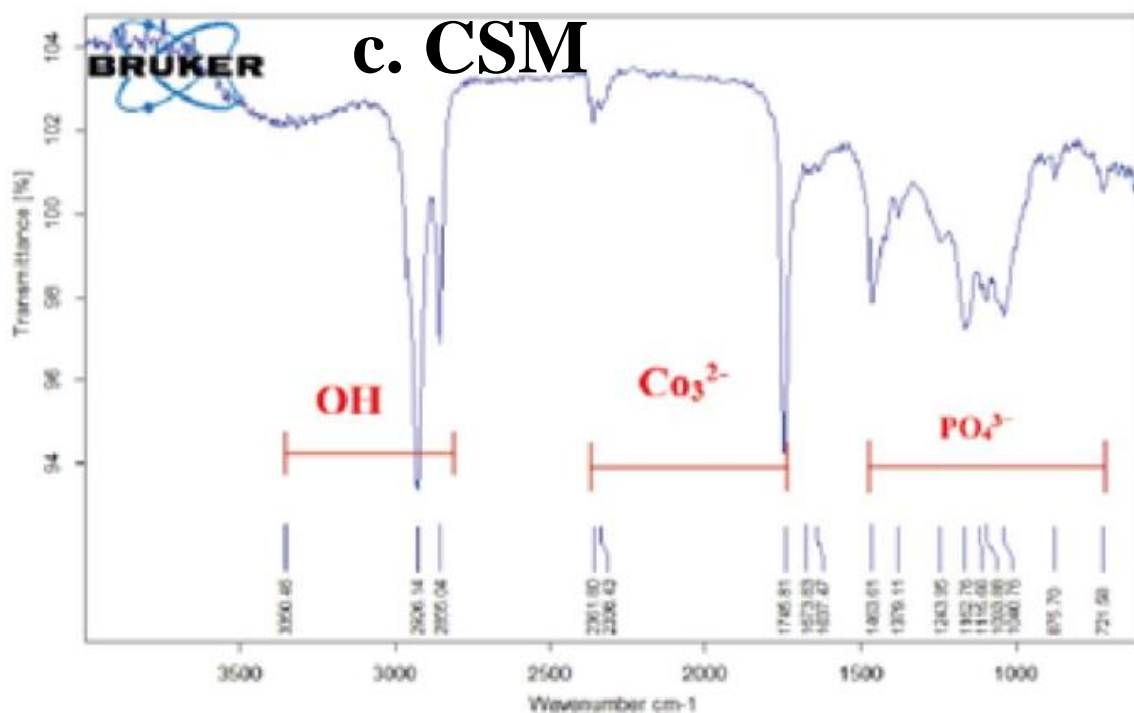


Figure 13 show the FTIR test for ESM FILM, FBM FILM, and CSM FILM

3.3 Atomic Force Microscopy AFM

To have full information about surface texture if samples after coating with natural hybrid composite materials and after covering with mastic layer AFM was preform as shown in the figure. Average surface roughness is shown in the table and figure. The roughness of the SS sample before the composite coating was 20.65 nm as shown in the texture after using the hybrid natural composites as a coating in the surface shape shown by the layer by varying the average surface roughness. The roughness was oscillating due to differences in the hydroxyapatite source which affects the whole properties of the component materials and as mentioned in the FE-SEM result. Since the hydroxyapatite granules extracted from the eggshell was very smooth and filled all the cavities and grooves in the surface of the stainless steel, we notice a high

reduction in the roughness where it became (8nm). Adding hydroxyapatite extracted from fish bones leads to the formation of grooves and large and high peaks, which leads to a very high average roughness (63). In addition to hydroxyapatite extracted from cockle shells and since it is formed on the surface in the form of piles, the average roughness is (36). When adding mastic powder to the coating materials, a significant decrease was observed in the average roughness, as the average roughness was (4.7, and 13) for samples (ESM, FBM, and CSM) respectively. This is because the mastic granules are very small, so they enter and fill all the cavities of the surface, which reduces the average roughness. the result shown in figure 16 and figure 17

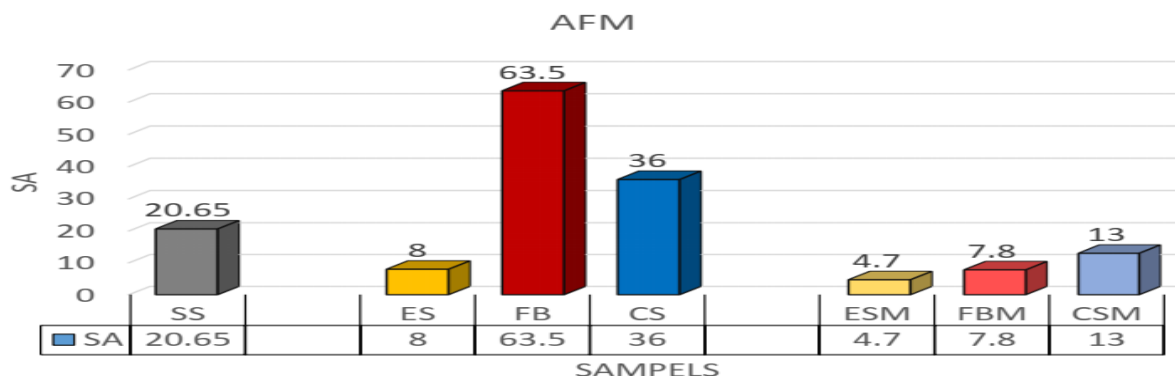
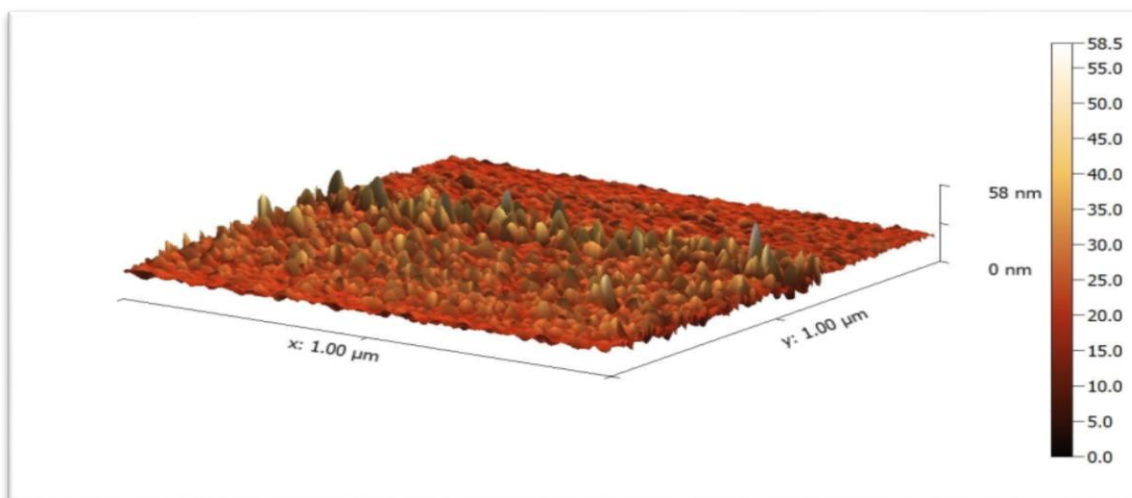
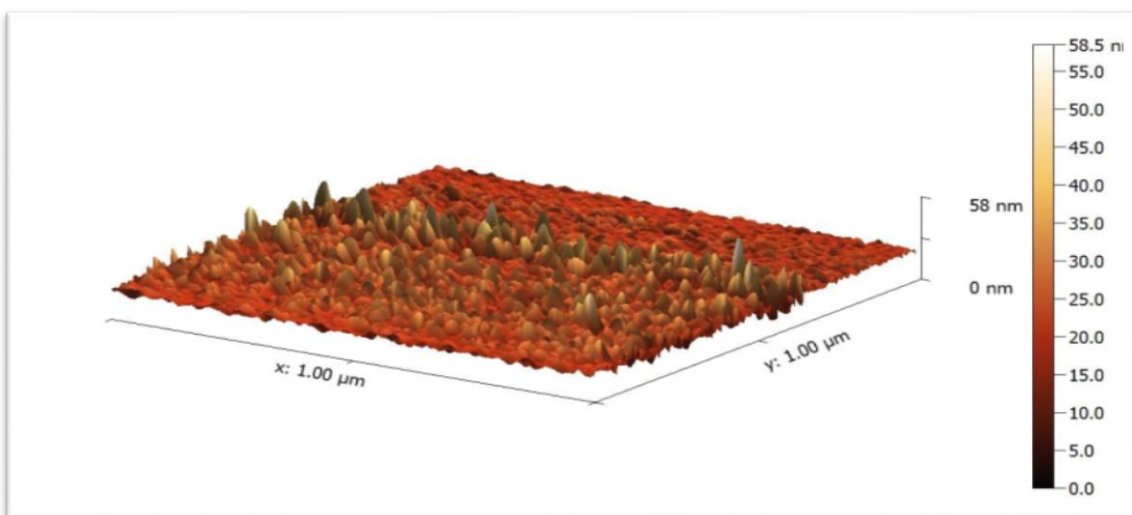


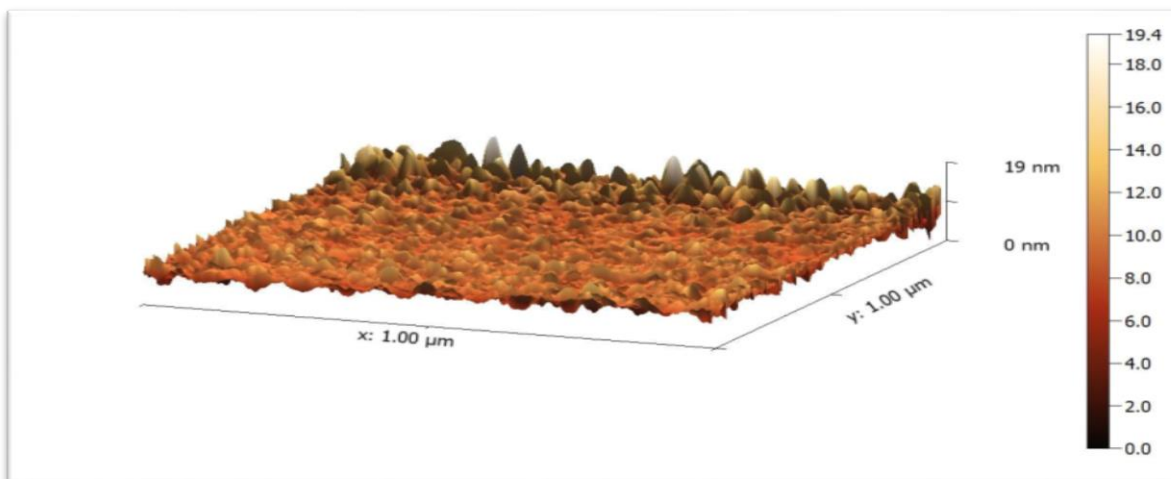
Figure 14 displays the values of the height's arithmetic mean and root mean square as well as the heights of peaks and valleys on the surface



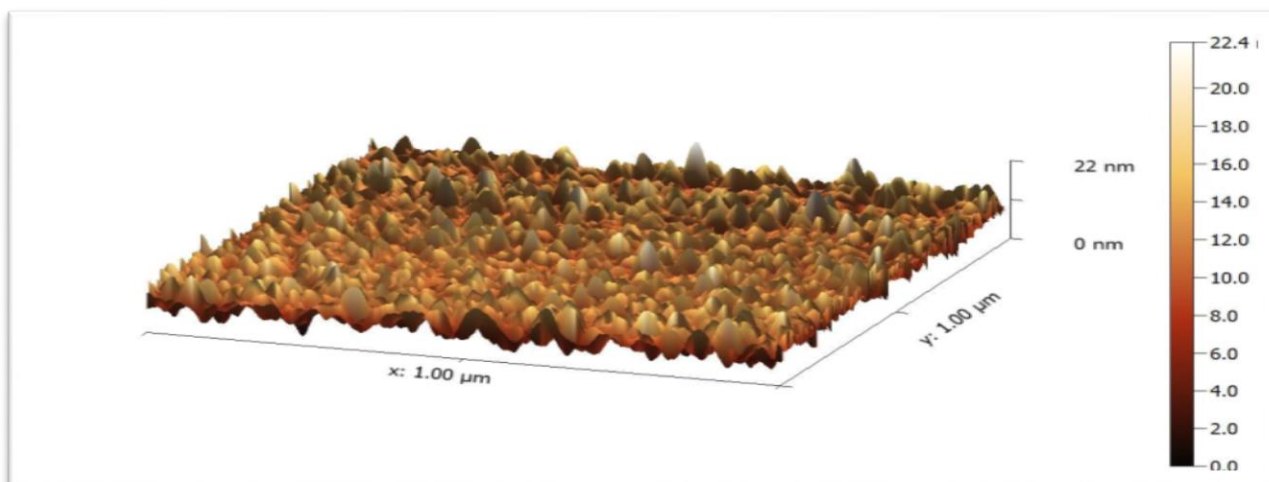
Three dimensional of samples ES



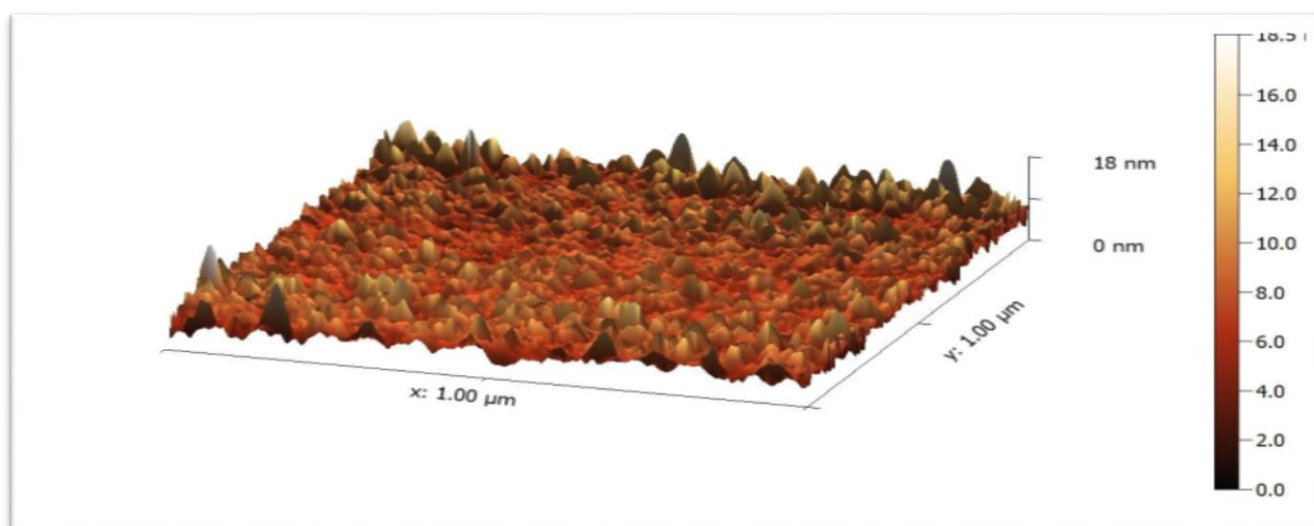
Three dimensional of samples FB



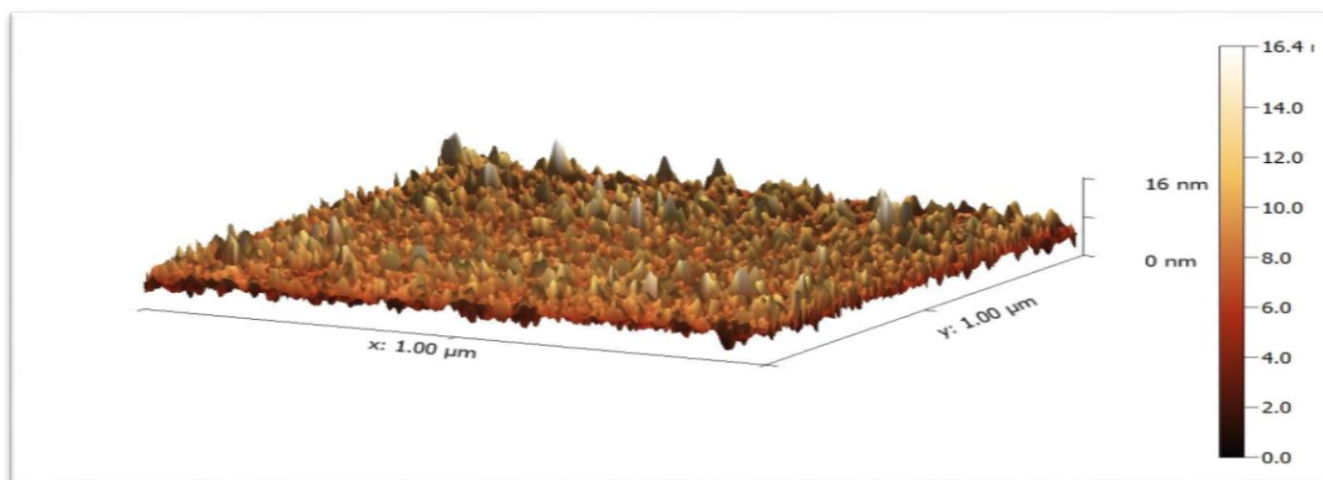
Three dimensional of samples CS



Three dimensional of samples ESM



Three dimensional of samples FBM



Three dimensional of samples CS

Figure 15 three-dimensional shape of samples (SS, ES, FB, CS, ESM, FBM, and CSM)

3.4 Contact Angle

Based on the observation of uncertainty, IT IS emphasize the behavior of hydroxyapatite in terms of being a hydrophilic or hydrophobic substance, depending on the various sources from which it is taken. Hydrophilic describes hydroxyapatite. The rate of dissolution, however, is frequently slow [7]. Though to varied degrees depending on the source of the extract, the addition of a natural polymer with water-soluble components and substances that enter the water from within its composition led to naturally formed hydroxyapatite exhibiting hydrophilic behavior. Because cockle shells have a shell structure that contains salts to a great extent, as described in the results, they have the best degree of hydrophilicity and therefore the best wetness. The hydroxyapatite from the eggshell, which is next, has a considerable degree of hydrophilicity due to the absence of any oily materials in the structure. Although it is important to

note that hydroxyapatite made from fish bones has a poor hydrophilicity, this is due to

According to the FE-SEM and XRD results, the hydroxyapatite structure contains oily compounds that insulate water and decrease the material's wettability. The hydrophilic property of the natural composite hybrid material made from various sources of hydroxyapatite was strengthened when mastic, a naturally occurring water-soluble resin, was added, as illustrated in figures 4.38 and 4.39. The hydroxyapatite isolated from eggshells displayed the best improvement because to its skeletal structure, which had mastic granules scattered inside of it, offering homogeneity in the structure and increasing the hydrophilic property. The construction of cockle shells does not contain pores within, which led to the dispersion of mastic granules on the surface but not to the extent seen in eggshells.

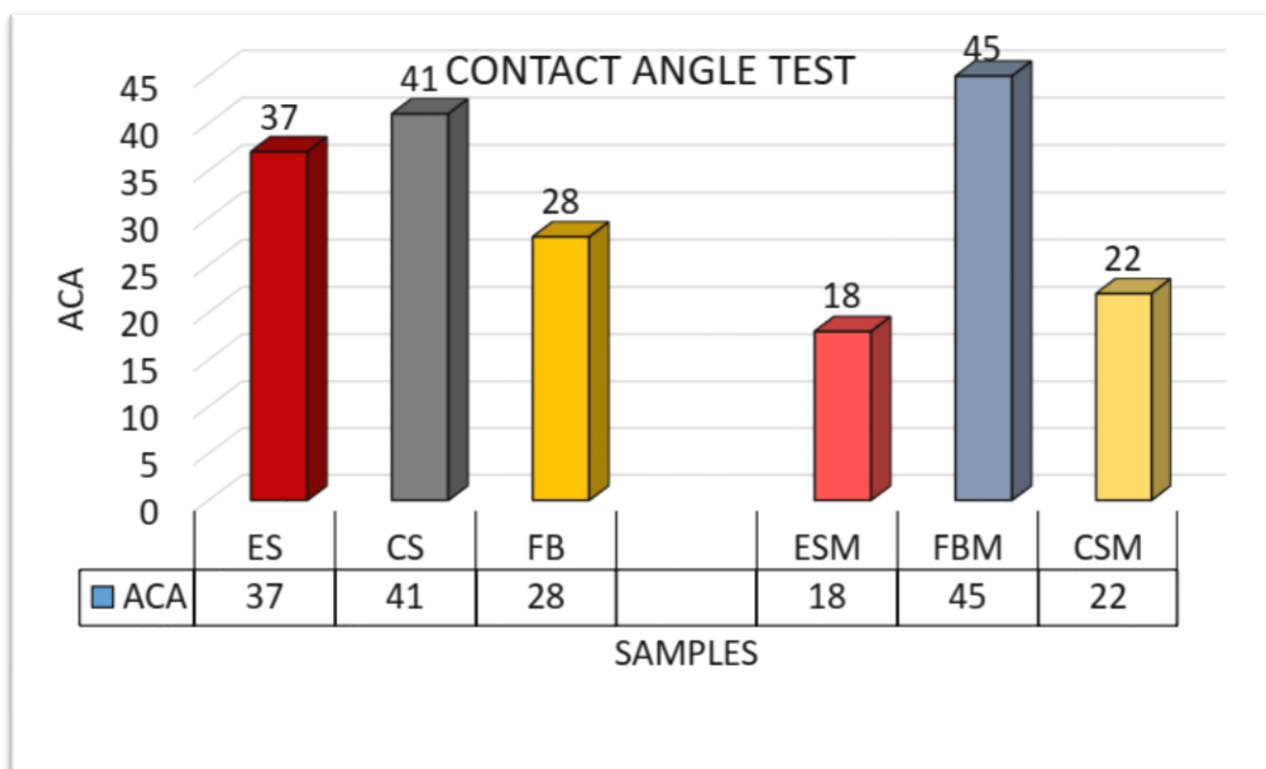


Figure 16 flow chart show contact angle test

3.5 MTT assay

MG-63 human fibroblast cultures' three-dimensional cell growth was observed utilizing mitochondrial dehydrogenase activity (MTT-assay) overexposure durations of (24, 48, and 72) hours. Three samples were investigated after being covered with a natural hybrid composite material derived from stainless steel, and the test was conducted on a stainless steel sample without any additives or surface treatments

(natural hydroxyapatite extract from eggshell, fishbone, and cockle shell, with natural polymer). The test was run on many samples including SS, ES, FB, SC, ESM, FBM, and CSM.

Due to the average toxicity range, which is suitable for all samples with the same difference in cell viability to samples surface composition, the result demonstrates that implant sample biocompatibility with cells.

After SS samples have been covered in a composite layer (natural polymer with hydroxyapatite extraction from eggshell, fishbone, and cockle shell). According to the MTT results, cell availability has increased for all samples with varying hydroxyapatite sources. Due to the active biological nature resulting in the active proliferation process, cell availability of ES and CS rises to 90%. Whereas fishbone is 88% (small change compared with SS sample).

This is because, in addition to the hydroxyapatite crystallinity noted in FE-SEM and XRD, the oily material component of the implant surface contains fishbone hydroxyapatite, which functions to provide cell attachment and result in

inhibiting the proliferation of process at the implant surface. Additionally, the separation of the hydroxyapatite granules from the cells results in less protein adhesion to the surface, which in turn results in less cell presence and less activation of the proliferation process.

Finally, coating the surface of the implants with mastic will promote cell availability, which will enhance the biocompatibility of the samples while protecting them from the environment. This has a major impact on protecting the surface from microbial attachment but has little influence on cell availability.

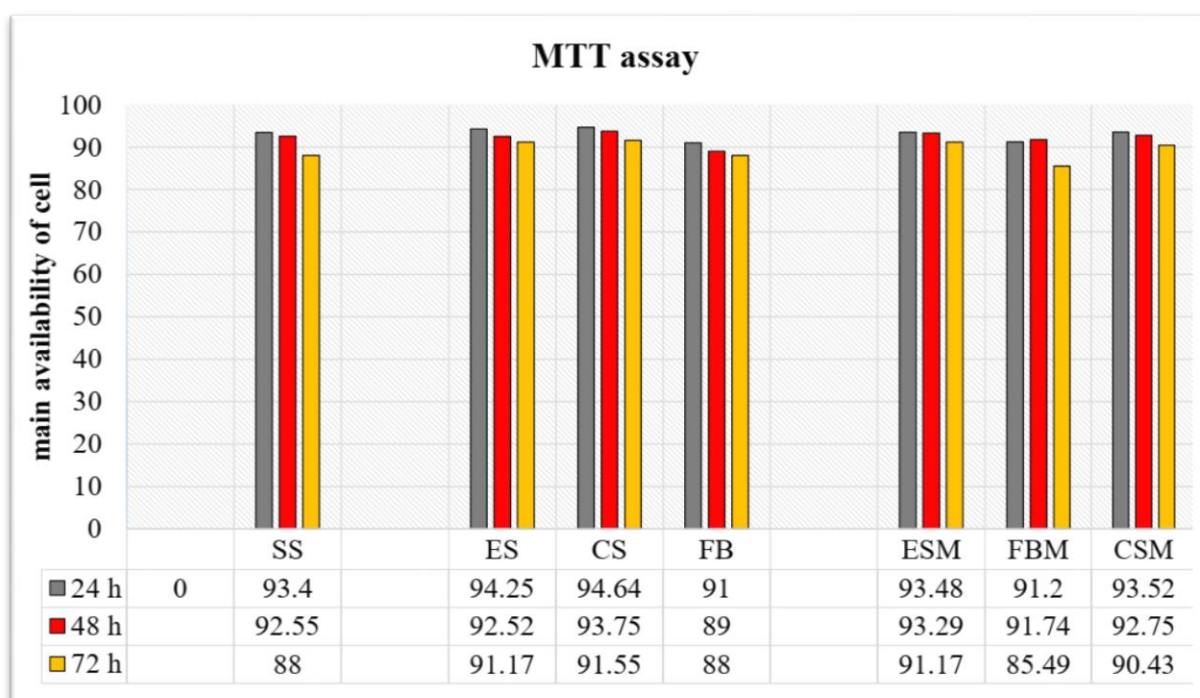


Figure 17 shows the flow chart for the MTT result

4. 4-COCLUSION

This research showed that it is possible to take advantage of natural waste that is not included in any actual applications

and convert it into effective biological materials of high quality and biocompatibility that can be used within the biological system. Thus, a link can be made between biomaterials and the development of sustainability.

REFERENCES

- [1] de Almeida, C. D., & Queirós, O. (2022). Special Issue “Novel Developments in the Bioproduction of Biochemicals and Biomaterials”. Applied Sciences, 12(20), 10631
- [2] Kumar Gupta, G., De, S., Franco, A., Balu, A. M., & Luque, R. (2015). Sustainable biomaterials: Current trends, challenges and applications. Molecules, 21(1), 48 .
- [3] Shi, P., Liu, M., Fan, F., Yu, C., Lu, W., & Du, M. (2018). Characterization of natural hydroxyapatite originated from fish bone and its biocompatibility with osteoblasts. Materials Science and Engineering: C, 90, 706-712.
- [4] Gergely, G., Wéber, F., Lukács, I., Illés, L., Tóth, A., Horváth, Z., ... & Balázs, C. (2010). Nano-hydroxyapatite preparation from biogenic raw materials. Open Chemistry, 8(2), 375-381.

- [5] R. Pereira, A. Tojeira, D. C. Vaz, A. Mendes, and P. Bártolo, "Preparation and characterization of films based on alginate and aloe vera," *Int. J. Polym. Anal. Charact.*, vol. 16, no. 7, pp. 449–464, 2011, doi: 10.1080/1023666X.2011.599923.
- [6] S. Bruni and V. Guglielmi, "Identification of archaeological triterpenic resins by the nonseparative techniques FTIR and ¹³C NMR: The case of Pistacia resin (mastic) in comparison with frankincense," *Spectrochim. Acta - Part A Mol. Biomol. Spectrosc.*, vol. 121, pp. 613–622, 2014, doi: 10.1016/j.saa.2013.10.098.
- [7] Y. Okabe, S. Kurihara, T. Yajima, Y. Seki, I. Nakamura, and I. Takano, "Formation of super-hydrophilic surface of hydroxyapatite by ion implantation and plasma treatment," *Surface and Coatings Technology*, vol. 196, no. 1-3 SPEC. ISS. pp. 303–306, 2005, doi: 10.1016/j.surfcoat.2004.08.190.